

Short Communication

Puff Pastry-like Co(OH)₂ Nano-flakes Grown on Nickel Foams for High-performance Supercapacitors

Shuaishuai Zhu^{1,§}, Yuming Dai^{1,*§}, Chuanxiang Zhang¹, Tianyu Zhang¹, Keyu Zhu¹, Yuhan Zeng¹, Ziyang He²

¹ Jiangsu Key Laboratory of Advanced Structural Materials and Application Technology, School of Materials Engineering, Nanjing Institute of Technology, Nanjing 211167, P.R. China

² Department of Industrial and Manufacturing System Engineering, Iowa State University, Ames, Iowa 50011, United States

*E-mail: Y.M.Dai@hotmail.com

§ Shuaishuai Zhu and Yuming Dai contributed equally.

Received: 11 September 2017 / Accepted: 6 November 2017 / Published: 16 December 2017

The unique puff pastry-like Co(OH)₂ nano-flakes were potentiostatic electrodeposited on the surface of Ni foams. The nano-flakes in the composite provides sufficient contact of active material with electrolyte and facilitates the adsorption/desorption of ions in the electrode solution. It exhibits a high specific capacitance of 2138 F/g at 5 mV/s, and the resistance is only 0.65 Ω. It also shows a good long-term stability of 80.5 % capacitance retention over 10000 charge/discharge cycles at 5 A/g.

Keywords: supercapacitors; cobalt hydroxide; electrodeposition; nanoflakes; energy storage and conversion

1. INTRODUCTION

Supercapacitors have attracted tremendous attentions for their advantages of the high power density, long cycle life, wide operation temperature range and improved safety in energy-storage devices in recent years [1-3]. They are promising in applications such as electric vehicles, military equipment, consumer electronic devices and power backup systems owing to the above advantages [4, 5]. Supercapacitors can be classified into electrical double layer capacitors (EDLs) and pseudocapacitors for the different storage mechanisms. The EDLs are dominated by diffusion and accumulation of electrostatic charge at the interface of electrolyte/electrode [6]. The pseudocapacitors are governed by highly reversible Faradaic reactions on the surface and in the bulk of the electrode materials [7]. Thus, the specific capacitance (SC) of the pseudocapacitors may achieve dozens even

hundreds times of the EDLs due to the above mechanisms [8, 9]. Consequently, the pseudocapacitors are gaining a growing number of researches [10, 11]. The active electrode materials which undergo pseudo-capacitance include transition metal oxides [12], hydroxides [13], sulphides [14], nitrides [15], conductive polymers [16].

Among numerous electrode materials for pseudocapacitors, cobalt hydroxide is a promising material due to its high theoretical SC (3460 F/g), excellent cyclic stability and low-cost [17]. However, the SC of Co(OH)_2 -based pseudocapacitors is still much lower than the theoretical value for the poor electrical conductivity and low electroactive areas. Nowadays, the Co(OH)_2 nanocrystals with various morphologies for supercapacitors prepared by using homogeneous precipitation method [18], hydrothermal method [19] and electrodeposition method [20] have been reported. The electrodeposition method is the most efficient and low-cost method for the preparation of Co(OH)_2 thin films among these methods.

Herein, the Nickel foams (NFs) were soaked with hydrochloric acid solution to obtain micro-grooves on the surface firstly. Then the parallel Co(OH)_2 nano-flakes were fabricated by two-electrode potentiostatic electrodeposition method on the pretreated NFs surface for the tip effect and the orientation growth. The cyclic voltammetry, galvanostatic charge/discharge and electrochemical impedance spectroscopy were used to study the electrochemical properties of the Co(OH)_2 /NFs composite.

2. EXPERIMENTAL SECTION

2.1 Preparation of the Co(OH)_2 /NFs composite

Nickel foam substrate with a size of 1 cm \times 3 cm was cleaned ultrasonically with acetone, hydrochloric acid solution, water and anhydrous ethanol, respectively. The electrodeposition was controlled by a battery analyzer (Neware BTS3000) with a two-electrode cell in 0.1 M $\text{Co(NO}_3)_2$ aqueous solution. The above Nickel foam piece is cathode, and a 1 cm \times 3 cm graphite sheet is anode. The deposition time is 120 s, and the deposition potential is invariable. After electrodeposition, the as-prepared Co(OH)_2 /NFs composites were ultrasonically cleaned in deionized water, and then dried thoroughly at room temperature. The mass of the Co(OH)_2 was tested by the Sartorius microbalance with ± 0.01 mg accuracy.

2.2 Structure Characterization

The structure of the as-prepared Co(OH)_2 were examined by X-ray diffraction (XRD, Rigaku Ultima-IV) with the Cu $K\alpha$ ($\lambda = 0.1514$ nm) as radiation source, Raman spectrometer (RS, Renishaw Invia) with an excitation wavelength of 514 nm, X-ray photoelectron spectroscopy (XPS, Thermo ESCA2000) using Al $K\alpha$ monochromatized radiation. The morphology of samples was observed by transmission electron microscopy (TEM, JEOL JEM-2100, 200 kV) and scanning electron microscopy (SEM, JEOL 6360LV, 10 kV).

2.3 Electrochemical Tests

The unique puff pastry-like $\text{Co}(\text{OH})_2$ nano-flakes electrodeposited on the pretreated NFs surface without binder or conductive agent were used as working electrodes directly. An electrochemical workstation (Ametek 2273) was used to measure the cyclic voltammetry (CV) and electrochemical impedance spectroscopy (EIS) using three-electrode mode in 2 M KOH aqueous solution at room temperature. The counter and reference electrodes were platinum foil (2 cm \times 2 cm) and Hg/HgO electrode, respectively. The potential range for CV tests was 0 to 0.5 V at scan rates of 5, 10, 15, 20 and 50 mV/s.

The EIS were tested from 100 KHz to 0.1 Hz, and the sine wave amplitude was 5 mV. A supercapacitor analyser (SCTS, Arbin) was used to study the galvanostatic measurements and capacitance retention with the two-electrode mode in 2 M KOH aqueous solution. The anode, the cathode and the separator film were $\text{Co}(\text{OH})_2/\text{NFs}$ sample, graphite sheet and polyethylene (PE) fibrous paper, respectively. The potential window of the tests is 0 to 0.5 V.

3. RESULTS AND DISCUSSION

3.1. Morphology Analyses

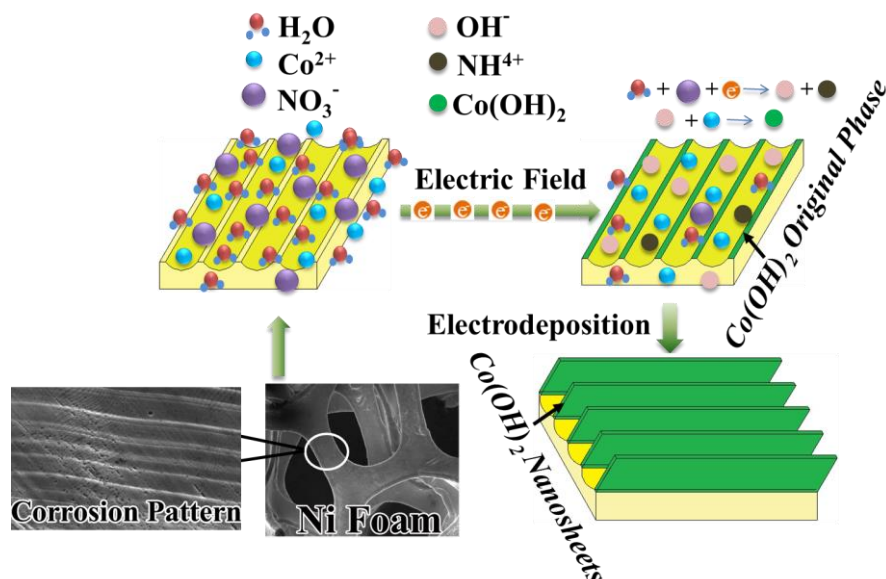
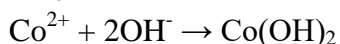
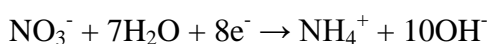


Figure 1. Schematic illustration of the fabrication process of $\text{Co}(\text{OH})_2$ puff pastry-like nano-flakes structure

The schematic illustration of the fabrication process of puff pastry-like $\text{Co}(\text{OH})_2$ nano-flakes is shown in Figure 1. The reaction of $\text{Co}(\text{OH})_2$ electrodeposition can be described as following equations [20].



Firstly, the water is ionized and generated OH^- ions, and the cathode attracts positively charged Co^{2+} ions to its surface because of electrostatic attraction in the electric field. Then the Co^{2+} ions chemically react with OH^- around the cathode to form $\text{Co}(\text{OH})_2$ nucleus and then deposit on the cathode. During the pretreatment process of the cathode (nickel foam), the parallel micro-grooves on the NFs surface were controlled by hydrochloric acid corrosion. The current density near the the groove walls is high for the tip effect [21], which promotes the electrodeposition of $\text{Co}(\text{OH})_2$ on the top of the groove walls. Some reports indicate that $\text{Co}(\text{OH})_2$ will grow in a preferred orientation during the process of electrodeposition [20,22,23], and the growth orientation of $\text{Co}(\text{OH})_2$ will be perpendicular to the plane of NFs. Consequently, the growth of $\text{Co}(\text{OH})_2$ is along the groove walls to form the parallel $\text{Co}(\text{OH})_2$ nano-flakes in our work.

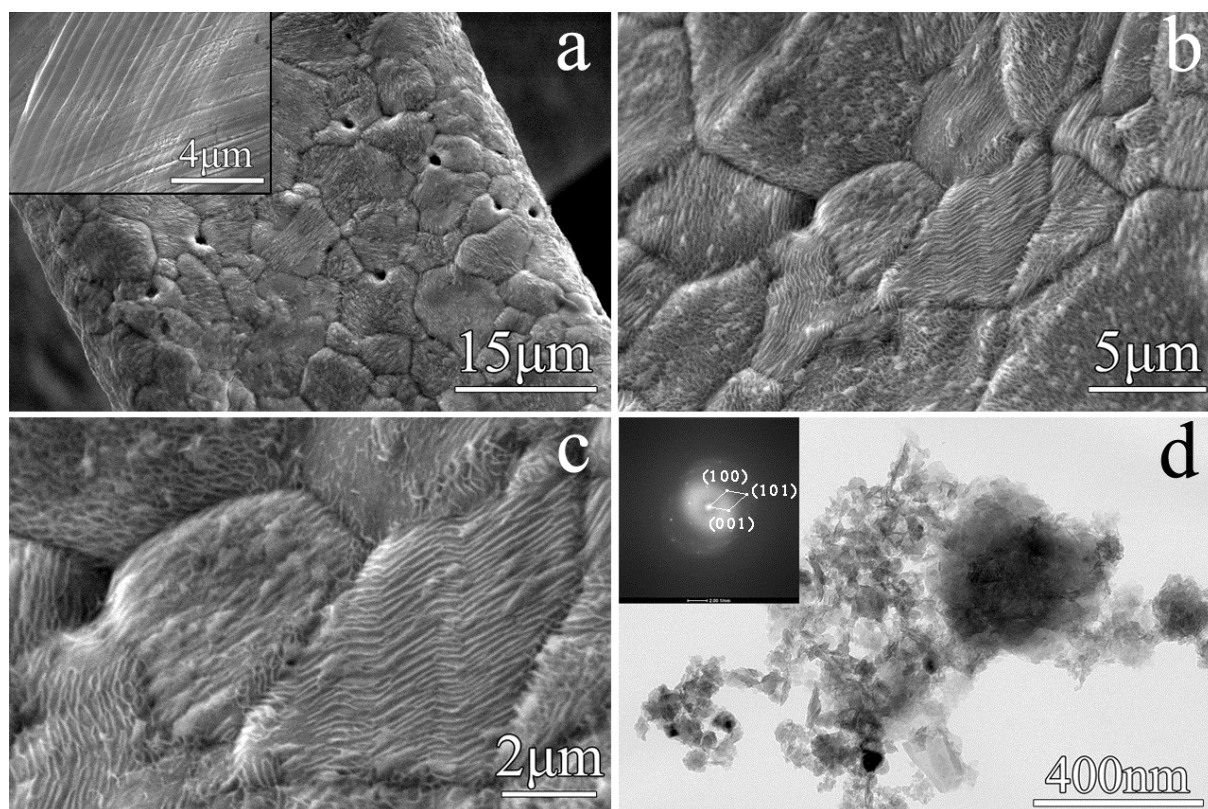


Figure 2. (a-c) SEM images at different magnifications, (d) TEM image and SAED pattern of the $\text{Co}(\text{OH})_2/\text{NFs}$ composite

Figure 2a is the macroscopic morphology of the optimal $\text{Co}(\text{OH})_2/\text{NFs}$ composite, it is obvious that the skeleton of NFs was densely covered with electrodeposition products. The morphology of the pretreated NFs surface (the inset of Figure 2a) shows that the parallel micro-grooves were eroded during the acid cleaning process. The magnification image (Figure 2b) indicates the electrodeposition products were parallel nano-flakes, which were different with other prepared $\text{Co}(\text{OH})_2$ with porous network structure [23,24]. This is due to the tip effect of the parallel micro-grooves and the orientation growth during the electrodeposition. The further magnification (Figure 2c) reveals that the spacing of nano-flakes is 150 ± 10 nm. The spaces between the nano-flakes can provide passageway for ionic conduction and electrolyte diffusion in the film bulk. And the nano-flakes structure provide higher

specific surface area of the film, thus increase its SC [25]. The TEM image (Figure 2d) of powder stripped from the as-product shows the Co(OH)_2 is consist of thin flakes. In a corresponding selected-area electron-diffraction (SAED) pattern (the inset of Figure 2d) shows symmetrical and clear electron diffraction spots, which is attributed to Co(OH)_2 .

3.2 Structure Analyses

Figure 3a shows XRD patterns of the $\text{Co(OH)}_2/\text{NFs}$ composite. The diffraction peaks at 18.9° , 33.4° , and 67.6° respectively correspond to the (001), (100), and (200) planes of $\alpha\text{-Co(OH)}_2$ (JCPDS No. PDF 30-0443). However, the intensity of diffraction peak decreased for the parallel Co(OH)_2 nano-flakes along the basal planes [26]. So the strongest diffraction peaks in Figure 3a was not pronounced, which is different with other prepared Co(OH)_2 [22-25]. In the Raman spectrum (Figure 3b) of the composite, the bands at 190.8, 471.3, 513.2, 608.3 and 674.3 cm^{-1} are induced by the vibration contraction of the Co-O bond and the polarization of the deformation of $-\text{OH}$ [27]. XPS survey spectra of the composite (Figure 3c) reveals that it has been detected peaks of $\text{Co } 2p_{1/2}$, $\text{Co } 2p_{3/2}$ and $\text{O } 1s$. Figure 3d is the high resolution spectra of $\text{Co } 2p$ of the composite. The results further confirm the coatings on the surface of as-product is pure Co(OH)_2 .

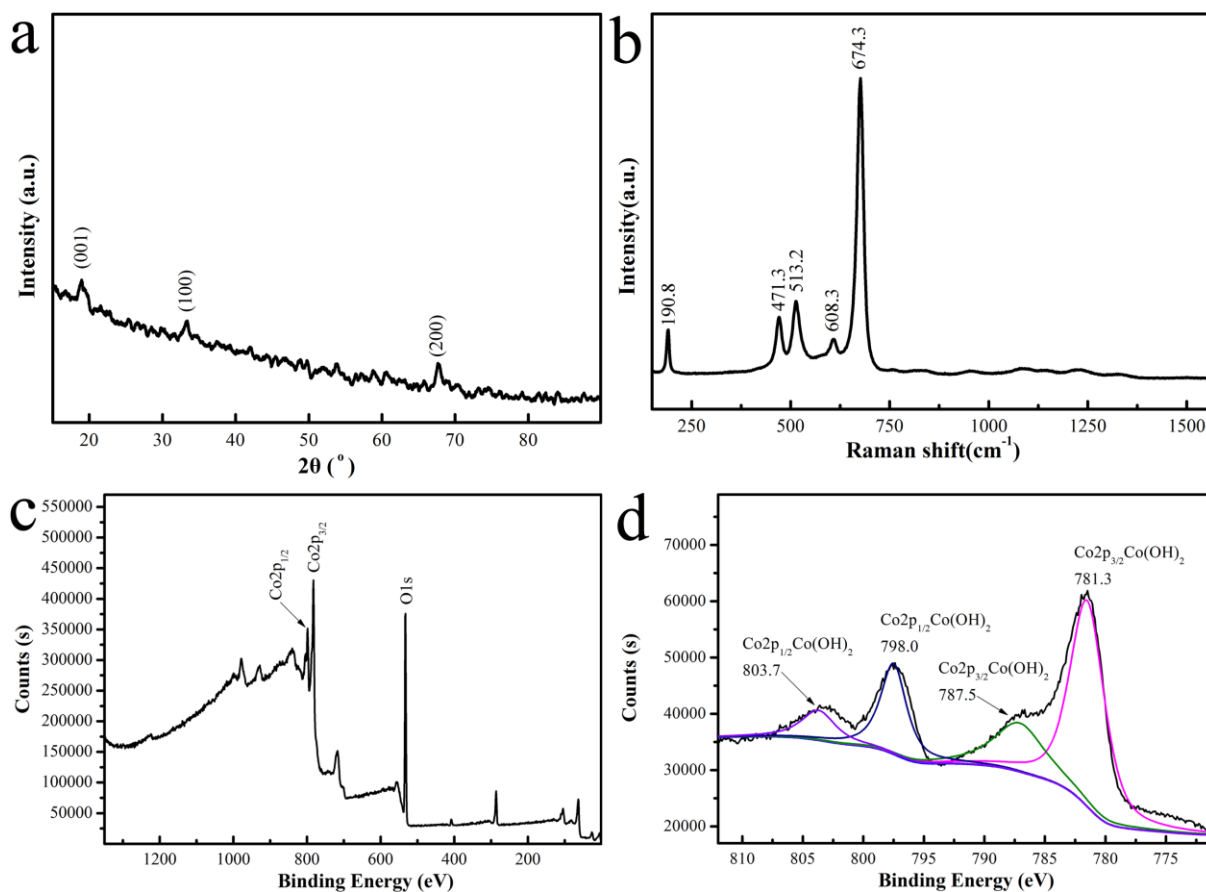


Figure 3. (a) XRD patterns, (b) Raman spectrum, (c) XPS survey and $\text{Co } 2p$ spectra of the powder stripped from the as-product

3.3 Electrochemical Analyses

The CV curves measured at scan rates from 5 to 50 mV s⁻¹ of the Co(OH)₂/NFs composite are shown in Figure 4a.

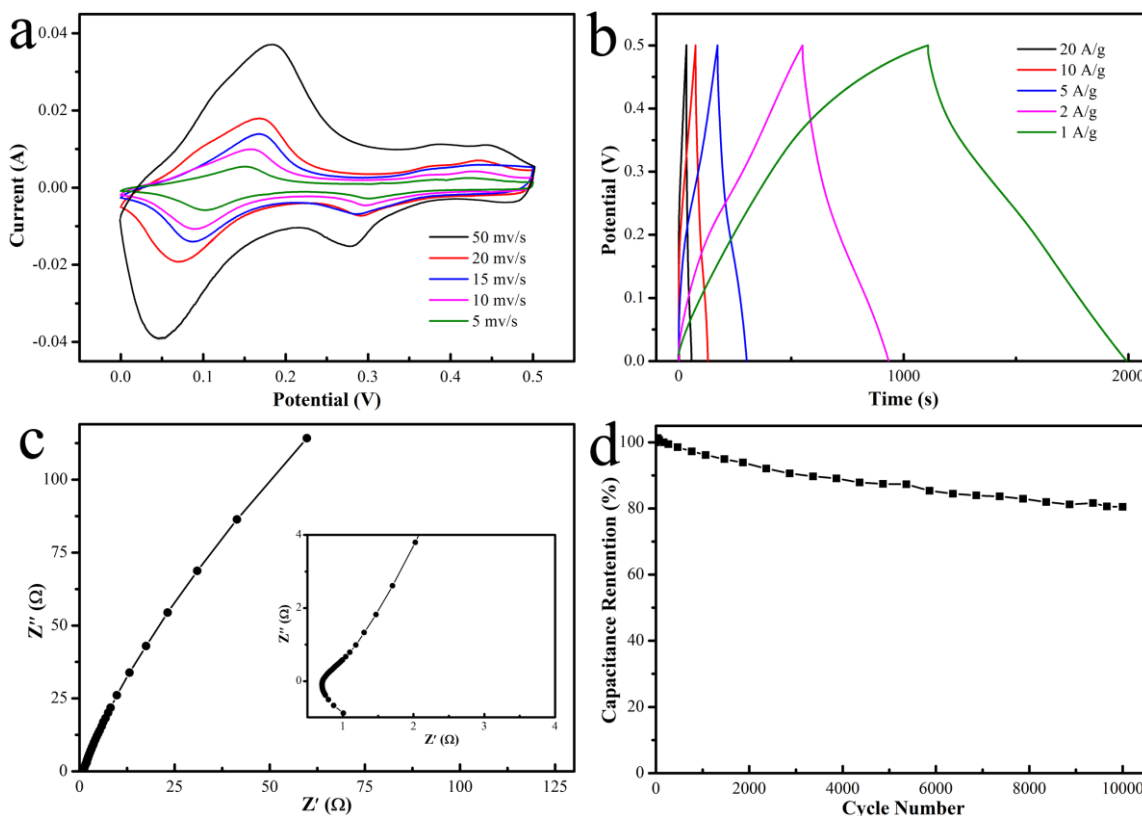
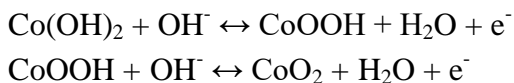


Figure 4. Electrochemical performance of the Co(OH)₂/NFs composite. (a) CV curves at various scan rates, (b) Charge/Discharge curve at different current densities, (c) EIS and (d) Capacitance retention at 5 A g⁻¹ over 10000 cycles

The shapes of the CV curves are not the ideal rectangular shape. According to the literatures [18-20,22,28], the four peaks on the single curve represent that two reversible redox processes occurred in the testing process. And the redox reactions on the surface of the composite will proceed as following equations.



The CV curves indicate that the anodic and cathodic peaks are symmetric, suggesting that the reversibility for the composite is excellent. The SC values of the as-products were calculated by the following equation.

$$\text{SC} = Q / (2vm\Delta V)$$

Where Q is the integral area of the CV curve, v is the scan rate, m is the mass of active material, and ΔV is the potential window. The SC of the Co(OH)₂/NFs composite is 2138, 1828, 1660, 1609 and 1392 F g⁻¹ at scan rates of 5, 10, 15, 20 and 50 mV s⁻¹, respectively. The SC decreases gradually with

the increasing of scan rate, the value at 50 mV s^{-1} is only a 35 % decrease compared with that at 5 mV s^{-1} , which imply a good high-current capability. The value of 2138 F g^{-1} is twice as much as the ultrathin Co-Co(OH)₂ composite nanoflakes on 3D nickel foam (1000 F g^{-1} at 5 mV s^{-1})[29]. The remarkable SC of the as-product is mainly contributed by the active Co(OH)₂ nano-flakes on the NFs surface. The puff pastry-like nano-flakes shown in Figure 2 ensure sufficient contact of active material with electrolyte and facilitate the adsorption/desorption of ions in the electrode solution. Accordingly, the excellent capacitance is acquired.

Figure 4b presents the typical galvanostatic charging/discharging plots for the Co(OH)₂/NFs composite, respectively, at various current densities of 1, 2, 5, 10 and 20 A g^{-1} , which is used to evaluate the electrochemical performance and estimate the stable potential windows of the composite. As shown in Figure 4b, there was no apparent instantaneous potential drop, which means that the conductivity of the composite is excellent. The SC can be calculated as 1768, 1533, 1298, 1106 and 930 F g^{-1} at current densities of 1, 2, 5, 10, 20 A g^{-1} , respectively. The value of 1768 F g^{-1} (at 1 A g^{-1}) is close to the single-layer Co(OH)₂ (2028 F g^{-1}) [17], and is higher than the NiCo₂S₄@Co(OH)₂ core-shell nanotube (1054.95 F g^{-1}) [30] and cobalt hydroxide carbonate/activated carbon nanocomposite (301.44 F g^{-1}) [31].

The EIS analysis (Figure 4c) indicates that the charge-transfer resistance of the composite is only 0.65Ω . Meanwhile, the straight line of the low frequency region reveals that the transport of ion/electron is rapid, and the insert picture in Figure 4c show that there is no impedance arc high frequency region meaning the resistance of the ion transfer is low. Therefore, the electrical conductivity and the SC of the composite is enhanced.

The cycling stability for the Co(OH)₂/NFs composite electrode is examined by continuous charge-discharge experiments for 10000 cycles at a current density of 5 A g^{-1} . As shown in Figure 4d, the composite has 80.5 % capacitance retention, indicating excellent long-term stability, which is attributed to the unique puff pastry-like structure, the parallel nano-flakes benefits the structural stability. Thus, these results reveal the ultrahigh specific capacitance and remarkable cyclic stability of the Co(OH)₂/NFs composite for high performance supercapacitors.

4. CONCLUSIONS

In this work, two-electrode potentiostatic electrodeposition on a battery analyzer has been utilized for the fabrication of Co(OH)₂/NFs composite. The SAED, XRD pattern, XPS and Raman spectrum indicate the deposit is pure Co(OH)₂. From the SEM images, the Co(OH)₂ presents unique puff pastry-like nano-flakes with spacing of $150 \pm 10 \text{ nm}$. The composite owns a high SC of 2138 F g^{-1} at 5 mV s^{-1} , and the resistance is only 0.65Ω . The composite also shows a good long-term stability of 80.5 % capacitance retention over 10000 charge/discharge cycles at 5 A g^{-1} . These results suggest that the unique puff pastry-like nano-flakes of the Co(OH)₂ nanostructure plays an important role in its excellent performance for supercapacitors. This is due to the parallel nano-falkes has good structure stability, ensure the sufficient contact of active material with electrolyte and facilitate the adsorption/desorption of ions in the electrode solution. Meanwhile, the electrical conductivity of the electrode material increased for the nickel substrate. Therefore, the Co(OH)₂/NFs composite with

unique puff pastry-like nano-flakes fabricated by this method can be used for applications in supercapacitors.

ACKNOWLEDGMENTS

This work was supported by the Outstanding Scientific and Technological Innovation Team in Colleges and Universities of Jiangsu Province, the National Natural Science Foundation of China (51402150), the High-level Talents Introduction Research Foundation of Nanjing Institute of Technology (ZKJ201404), the Scientific Research Foundation of Nanjing Institute of Technology (CKJA201502, JCYJ201606), the Natural Science Foundation of Jiangsu Province (BK20140763) and the Practice Innovation Program for College Students of Jiangsu Province (201711276040Y).

References

1. Y. Ruan, J. Jiang, and H. Wan, *J. Power Sources*, 301(2016)122.
2. Q. Wang, L. Zhu, and L. Sun, *J. Mater. Chem. A*, 3(2015)982.
3. C. Zhang, H. Yin, and M. Han, *ACS Nano*, 8(2014)3761.
4. Q. Li, W. Chen, and Z. Liu, *J. Power Sources*, 279(2015)267.
5. N. Padmanathan, S. Selladurai, and K. M. Razeeb, *RSC Adv.*, 5(2015)12700.
6. H. B. Li, M. H. Yu, F. X. Wang, P. Liu, Y. Liang, J. Xiao, C. X. Wang, Y. X. Tong, and G. W. Yang, *Nat. Commun.*, 4(2013)1894.
7. M. F. Dupont, and S. W. Donne, *J. Electrochem. Soc.*, 163(2016)A888.
8. W. Jiang, D. Yu, and Q. Zhang, *Adv. Funct. Mater.*, 25(2015)1063.
9. W. Wei, X. Cui, W. Chen, and D.G. Ivey, *Chem. Soc. Rev.*, 40(2011)1697.
10. L. Cao, S. Yang, and W. Gao, *Small*, 9(2013)2905.
11. J. Wang, X. Zhang, and Q. Wei, *Nano Energy*, 19(2016)222.
12. S. Zhuang, X. Xu, and B. Feng, *Acs Appl. Mater. Inter.*, 6(2013)613.
13. J. Kang, A. Hirata, and H. J. Qiu, *Adv. Mater.*, 26(2014)269.
14. P. Xu, J. Liu, and P. Yan, *J. Mater. Chem. A*, 4(2016)4920.
15. S. Wang, L. Zhang, and C. Sun, *Adv. Mater.*, 28(2016)3768.
16. J. Ma, Y.F. Liu, Z.H. Hu, and Z.J. Xu, *Ionics*, 19(2013)1405.
17. S. Gao, Y. Sun, F. Lei, and L. Liang, *Angew Chem. Int. Edit*, 53(2014)12789.
18. M. Li, J. P. Cheng, and J. Wang, *Electrochim Acta*, 206(2016)108.
19. M. Qorbani, N. Naseri, A. Z. Moshfegh, *ACS Appl. Mater. Inter.*, 7(2015)11172.
20. W. J. Zhou, M. W. Xu, D. D. Zhao, C. L. Xu, and H. L. Li, *Micropor. Mesopor. Mat.*, 117(2009)55.
21. Y. Lei, B. Daffos, and P. L. Taberna, *Electrochim Acta*, 55(2010)7454.
22. C. Zhao, W. Xin, S. Wang, H. Wang, Y. Yang, and W. Zheng, *Mater. Res. Bull.*, 48(2013)3189.
23. Y. Q. Zhang, X. H. Xia, J. Kang, and J. P. Tu, *Chinese Sci. Bull.*, 57(2012)4215.
24. J. A. Koza, C. M. Hull, Y. C. Liu, and J. A. Switzer, *Chem. Mater.*, 25(2013)1922.
25. M. Aghazadeh, A. Rashidi, P. Norouzi, and M. G. Maragheh, *Int. J. Electrochem. Sc.*, 11(2016) 11016.
26. L. B. Kong, M. C. Liu, J. W. Lang, M. Liu, Y. C. Luo, and L. Kang, *J. Solid State Electr.*, 15(2011) 571.
27. Y. C. Liu, J. A. Koza, and J. A. Switzer, *Electrochim Acta*, 140(2014) 359.
28. T. Nguyen, M. Boudard, M. J. Carmezim, and M. F. Montemor, *Sci. Rep.*, 7(2017)39980.
29. J. Gou, S. Xie, Y. Liu, and C. Liu, *Electrochimica Acta*, 210(2016)915.
30. Z. Yu, Z. Cheng, and S. R. Majid, *Chem. Commun.*, 51(2015)1689.
31. R. Li, S. Wang, and Z. Huang, *J. of Power Sources*, 312(2016)156.

32. T. M. Masikhwa, J. K. Dangbegnon, and A. Bello, *J. Phys. Chem. Solids*, 88(2016)60.

© 2018 The Authors. Published by ESG (www.electrochemsci.org). This article is an open access article distributed under the terms and conditions of the Creative Commons Attribution license (<http://creativecommons.org/licenses/by/4.0/>).